ISBN: 978-3-95450-227-1 ISSN: 2673-5490 doi:10.18429/JACoW-IPAC2022-WEPOTK013

DIRECT IMPEDANCE MEASUREMENT OF THE CERN PS BOOSTER FINEMET CAVITIES

S. Albright*, M. E. Angoletta, D. Barrientos, A. Findlay, M. Jaussi, J. Molendijk
CERN, Geneva, Switzerland

Abstract

Over CERN's Long Shutdown 2, the conventional ferrite-loaded cavities of the PS Booster were replaced with wide-band Finemet-loaded cavities. The Finemet cavities bring many operational advantages, but also represent a significant broadband impedance source. The impedance is mitigated by servo loops, which suppress the induced voltage, reducing the impedance as seen by the beam. Accurately including the impedance of the cavity and the effect of the servoloops in longitudinal tracking simulations is essential to predict the performance with beam.

This paper discusses the results of a measurement campaign, which is intended to give a direct measurement of the cavity impedance. Using the detected voltage and the measured beam profile, the cavity impedance can be inferred and used to improve beam dynamics modelling.

INTRODUCTION

The CERN PS Booster is the first synchrotron in the LHC proton injection chain. During Long Shutdown 2 (LS2), significant upgrades were implemented, which included replacing the ferrite-loaded cavities with Finemet-loaded cavities.

In each PSB ring, there are three nominally identical accelerating stations in sectors 5, 7 and 13. Each cavity is composed of 12 cells, which are assumed to have identical impedance. Each cell has a dedicated solid-state amplifier, which includes a fast feedback loop for impedance reduction. The amplifiers drive the two sides of the accelerating gap in anti-phase, causing it to act like a double $\lambda/4$-resonator.

In tracking simulations, an impedance model derived from S-parameter measurements was used. Figure 1 shows the absolute impedance from 0.5 MHz to 100 MHz [1]. The coloured bands in Fig. 1 indicate the frequency range of harmonics 1, 2 and 10, which are the ones most commonly used in operation. This study is focused on the impedance peak at approximately 19 MHz, indicated by the vertical red line in Fig. 1. In simulations, this peak was shown to cause longitudinal instabilities, potentially limiting the intensity reach [2].

The PSB provides beams covering a very large range of intensities with $O(10^9 \rightarrow 10^{13})$ protons per bunch and longitudinal emittances in the range from 0.3 eVs to 3.0 eVs. New beam production schemes, suited to the upgraded RF systems, were designed for the required PSB beam types [3]. During post-LS2 beam commissioning, it was found that the beam stability did not match predictions, therefore the production schemes were adapted [4]. The root causes

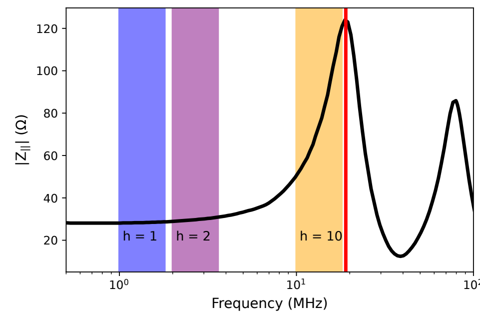

Figure 1: The absolute impedance of a single Finemet cell, the vertical red line is at 19 MHz and the coloured bands indicate the frequency spans of revolution harmonics 1, 2 and 10. Each cell is assumed to be identical in all cavities.

of the discrepancy are still under investigation, but possibly the impedance model applied in simulations is inaccurate. As the Finemet cavities are the dominant longitudinal impedance source, they were the first component to be studied, and this paper describes beam-based measurements of the cavity impedance.

Low Level RF (LLRF) servoloops suppress induced voltage for $h \leq 16$. When the frequency of a harmonic passes 20 MHz, the corresponding servoloop will open [5]. The resulting coupling impedance therefore depends on both the servoloop action and the open loop impedance. During commissioning in 2020, it was found that upgrades to the amplifiers were needed, which would also modify the open loop impedance [6]. For the results presented here, the cavities in sector 5 of all rings were therefore measured with beam in open loop, which includes two cavities with the original amplifiers (rings 1 and 2) and two with the upgraded amplifiers (rings 3 and 4). In the long term, all other sectors will also be measured in this way.

METHOD

Accelerator Configuration

To adequately identify the amplitude and location of the impedance peak, it is essential to maximise the beam power in the relevant frequency range. Therefore, a special beam was prepared to increase the beam power in the 10 MHz to 30 MHz range by adding extra RF voltage at the 10^{th} harmonic. Figure 2 gives the beam spectrum in this range with and without the $h = 10$ contribution, which shows the increased beam power at high frequency.

The voltage in all cells is summed and the result, referred to as the gap return signal, is used for measurements [5]. The

* simon.albright@cern.ch

ISBN: 978-3-95450-227-1 ISSN: 2673-5490 doi:10.18429/JACoW-IPAC2022-WEPOTK013

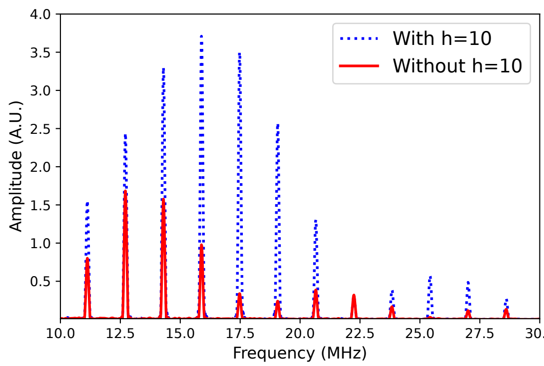

Figure 2: Beam spectra from 10 MHz to 30 MHz in pure $h = 1$ (solid red line) and with additional voltage at $h = 10$ (dotted blue line).

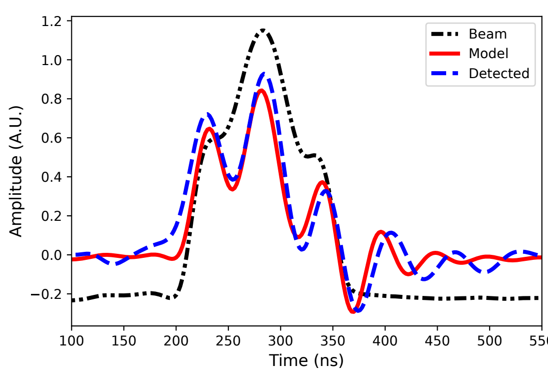

Figure 3: Measured beam profile (black dash-dot line) and the corresponding measured (blue dashed line) and simulated (red line) induced voltage.

gap return has approximately constant amplitude response in the frequency range of interest. To allow the full impedance to be measured, the sector 5 cavity servoloops were opened to prevent any compensation of induced voltage. Figure 3 shows an example measured beam profile and gap return, together with the modelled induced voltage.

Measurement

In the frequency domain, the beam induced voltage due to a given impedance is

$$V_{ind} = Z_{||} \times \lambda, \tag{1}$$

where V_{ind} is the induced voltage, $Z_{||}$ the longitudinal impedance, and λ the longitudinal line density. V_{ind} and λ were measured in the time domain then Fourier transformed to calculate $Z_{||}$.

A single bunch with small longitudinal emittance (0.3 eVs) was accelerated at low intensity ($2 \cdot 10^{11}$ protons). This ensured the beam remained stable longitudinally, but was short enough to sample the part of the impedance under consideration.

The beam profiles are measured by a wide-band wall current monitor, which is connected to the surface and split to the acquisition systems with a bandwidth well beyond the relevant frequency range. The beam profile and gap return signals were digitised at a sampling rate of 500 MS/s, which gives a significantly higher Nyquist frequency than required for the frequencies of interest. The high sampling rate avoided any risk of aliasing artifacts from higher frequency components of the beam spectrum.

An additional consideration in the booster is the relatively large revolution frequency swing, from about 1 MHz at injection to about 1.8 MHz at extraction. To mitigate its impact on the measurements, a short (100 ms) section of data was taken near the end of the cycle, which gave a frequency swing from 1.59 MHz to 1.74 MHz during the measurement window. To further limit the effect of the sweeping frequency, the Fourier transform was taken on sections of data 2^{16} samples long, equivalent to about 131 μs. Therefore, from the start to end of each section, the change in revolution frequency was 1.9 kHz or below and therefore the broadening of the spectrum could be neglected.

RESULTS

The spectrograms of the beam and gap return signals are shown in Fig. 4a and Fig. 4b respectively. By calculating the ratio of the gap return and beam spectral lines for each harmonic, the absolute cavity impedance can be directly determined.

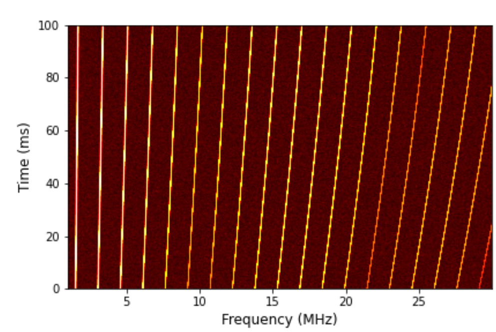

(a) Beam signal spectrogram

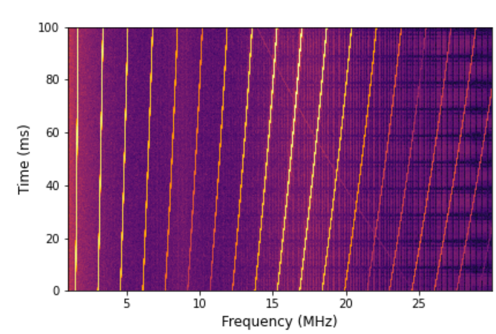

(b) Gap return signal spectrogram

Figure 4: Spectrograms of the beam and gap return signals from ring 1 over the full measurement time from 1 MHz to 30 MHz.

ISBN: 978-3-95450-227-1 ISSN: 2673-5490 doi:10.18429/JACoW-IPAC2022-WEPOTK013

The measured impedance for the sector 5 cavity in all rings is plotted in Fig. 5. From twenty cycles, the maximum and minimum impedance measured at each harmonic was used to define the shaded envelope, the central line indicates the average.

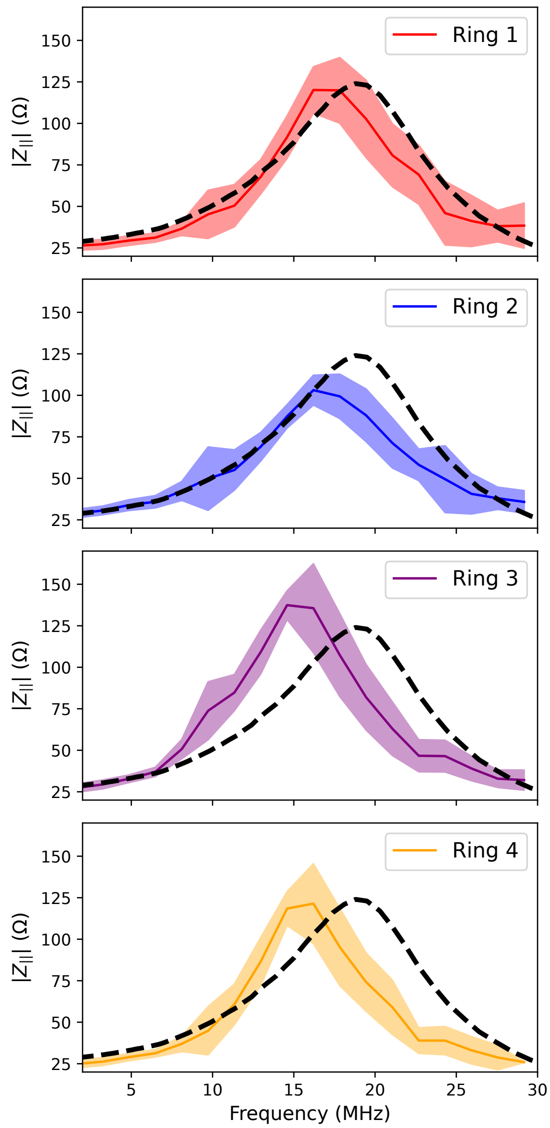

Figure 5: Comparison of the measured and modeled impedance in the 2 MHz to 30 MHz range for a single Finemet cell (Fig. 1). For each ring, the average measured impedance is given by the solid line, the shaded region represents the spread from twenty shots.

For all cavities, the peak of the impedance is at lower frequency than expected from the model. In rings 1 and 2, the peak is at approximately 17 MHz, in rings 3 and 4, with the upgraded amplifiers, it is at approximately 15 MHz. In comparing the four cavities, it is particularly noteworthy that rings 3 and 4 show a slightly increased impedance at low frequency, and a decrease at high frequency compared to rings 1 and 2. The amplifier upgrades were expected to increase the maximum impedance in this frequency range [6], which is confirmed by these measurements.

DISCUSSION AND FUTURE WORK

Comparing the measured impedance in ring 1 to ring 2, and ring 3 to ring 4 shows small differences between cavities with the same amplifiers. However, this may be due to measurement uncertainty. The differences between each cavity and the impedance model are much more significant. The impedance in the frequency range considered here was predicted to be the dominant factor in the longitudinal instability threshold. Therefore, this difference may be a factor to explain unexpected stability behaviour observed during beam commissioning..

The impedance being lower than modeled above about 18 MHz is likely to be beneficial for beam stability. However, the increased impedance around 15 MHz with the new amplifiers may have a negative effect. Whilst the LLRF servoloops significantly reduce the beam induced voltage, a larger than predicted impedance also implies a larger than predicted residual voltage.

As shown in [7], the gap return signal has a cavity dependent error of 8-18%, with a small frequency dependence. In future analysis, a more accurate calibration of the detected voltage will therefore be included to improve the accuracy of the results.

To remove the need for sectioning the measured data, it may be possible to use a short intermediate plateau at a specified revolution frequency. Then, the data can be acquired for the duration of that plateau, which will simplify the analysis.

The signal-to-noise ratio above 20 MHz is quite low, even with the $h = 10$ contribution. Operationally, the impedance at these frequencies is particularly critical as the servoloops do not act above 20 MHz. Therefore, in future measurements a spectrum analyzer will be used to increase the dynamic range.

CONCLUSION

The beam coupling impedances of the four Finemet cavities in sector 5 of the PSB have been measured. Two of these cavities (rings 1 and 2) feature the amplifiers originally installed during LS2 and two of them (rings 3 and 4) are equipped with upgraded. The measurements with beam show a slight increase in the maximum impedance with the new amplifiers, as expected from [6], and in all cases there is a clear discrepancy with respect to the impedance model used to predict accelerator performance.

More measurements are planned for the future, which will improve the accuracy of the results at high frequency and include the cavities in the remaining sectors. The results will then be incorporated into a refined longitudinal impedance model for tracking simulations. The new impedance model will then be used to continue studying the discrepancy between observed longitudinal instabilities between simulation and measurements.

ISBN: 978-3-95450-227-1 ISSN: 2673-5490 doi:10.18429/JACoW-IPAC2022-WEPOTK013

REFERENCES

[1] M. M. Paoluzzi *et al.*, “Design of the New Wideband RF System for the CERN PS Booster”, in *Proc. IPAC’16*, Busan, Korea, May 2016, pp. 441–443. doi:10.18429/JACoW-IPAC2016-MOPMW024

[2] D. Quartullo, “Simulations of RF beam manipulations including intensity effects for CERN PSB and SPS upgrades”, PhD. Thesis, Istituto Nazionale di Fisica Nucleare (INFN) and "Sapienza" Universita di Roma, Rome, Italy, 2019

[3] S. C. P. Albright, F. Antoniou, F. Asvesta, H. Bartosik, C. Bracco, and E. Renner, “New Longitudinal Beam Production Methods in the CERN Proton Synchrotron Booster”, in *Proc. IPAC’21*, Campinas, Brazil, May 2021, pp. 4130–4133. doi:10.18429/JACoW-IPAC2021-THPAB183

[4] S. C. P. Albright, M. E. Angoletta, D. Barrientos, A. Findlay, M. Jaussi, and J. C. Molendijk, “Commissioning the New LLRF System of the CERN PS Booster”, presented at IPAC’22, Bangkok, Thailand, Jun. 2022, paper WEPOTK012, this conference.

[5] D. Barrientos, S. C. P. Albright, M. E. Angoletta, A. Findlay, M. Jaussi, and J. C. Molendijk, “A New Beam Loading Compensation and Blowup Control System Using Multi-Harmonic Digital Feedback Loops in the CERN Proton Synchrotron Booster”, presented at IPAC’22, Bangkok, Thailand, Jun. 2022, paper TUPOST024, this conference.

[6] G. G. Gnemmi, S. Energico, M. Haase, M. M. Paoluzzi, and C. Rossi, “One Year of Operation of the New Wideband RF System of the Proton Synchrotron Booster”, presented at the IPAC’22, Bangkok, Thailand, Jun. 2022, paper TUPOTK055.

[7] D. Quartullo, S. C. P. Albright, and H. Damerau, “Frequency-Dependent RF Voltage Calibration Using Longitudinal Tomography in the CERN PSB”, presented at the IPAC’22, Bangkok, Thailand, Jun. 2022, paper TUPOST006.